Theoretical Study of Intramolecular Hydrogen Bonding and Molecular Geometry of 2-Trifluoromethylphenol

ATTILA KOVÁCS

Research Group for Technical Analytical Chemistry of the Hungarian Academy of Sciences at the Institute of General and Analytical Chemistry of the Budapest Technical University, H-1521 Budapest, Hungary

ISTVÁN KOLOSSVÁRY

Department of Chemical Information Technology of the Budapest Technical University, H-1521 Budapest, Hungary

GÁBOR I. CSONKA

Department of Inorganic Chemistry of the Budapest Technical University, H-1521 Budapest, Hungary

ISTVÁN HARGITTAI*

Institute of General and Analytical Chemistry of the Budapest Technical University, and Structural Chemistry Research Group of the Hungarian Academy of Sciences at Eötvös University, H-1521 Budapest, Hungary

Received 4 October 1995; accepted 9 February 1996

ABSTRACT

The conformational behavior of 2-trifluoromethylphenol was investigated by means of theoretical calculations. Four characteristic structures have been found on the potential energy hypersurface of the compound: *anti* form (local minimum), in which the hydroxy hydrogen points away from the trifluoromethyl group; and three *syn* forms (the hydrogen points towards the trifluoromethyl group), with different trifluoromethyl torsions (global minimum, one low and another one high lying saddle-point). The geometry of these conformers were optimized by *ab initio* calculations using 6-31G** basis set. The effects of electron correlation were investigated by MP2 and various DFT methods. To investigate the intramolecular interaction in the *syn* forms, the electron density distribution was calculated at the MP2 level of theory. In the structure

*Author to whom all correspondence should be addressed.

Journal of Computational Chemistry, Vol. 17, No. 16, 1804–1819 (1996)

CCC 0192-8651 / 96 / 161804-16

corresponding to the global minimum at the MP2/6-31G** level a *bond critical point* was found in Bader's sense between the hydroxy hydrogen and a fluorine of the trifluoromethyl group indicating hydrogen bonding interaction. The length of the hydrogen bond, 1.98 Å, corresponds to medium strength interaction. The O—H bond is slightly twisted and the C—F bond, interacting with it, is considerably twisted out of the plane of the benzene ring to the same side of the ring. The most pronounced geometrical consequence of the hydrogen bond is the 0.02-Å lengthening of the C—F bond participating in its formation. All the other geometrical changes in 2-trifluoromethylphenol, as compared with trifluoromethylbenzene and phenol, are also consistent with the phenomenon of resonance-assisted hydrogen bonding.

Introduction

The possibility of intramolecular hydrogen bonding makes the conformation of 2-trifluoromethylphenol (**1**) especially interesting. Some principal structures are summarized in Figure 1:

1a: *Anti* form. The hydroxy hydrogen points away ($\Theta_2 = 180°$) from the trifluoromethyl group, one of the C—F bonds is in the plane of the benzene ring, pointing away from the hydroxy group ($\Theta_1 \sim 60°$), C_s symmetry. Θ_1 is 0° when $F_{10}—C_9—C_2—C_1$ is *syn*, and Θ_2 is 0° when $H—O—C_1—C_2$ is *syn*.

1b: *Syn* form. The O—H bond and one of the C—F bonds are in the plane of the benzene ring, facing each other, C_s symmetry.

1c: *Syn* form, $\Theta_1 \sim 60°$, $\Theta_2 = 0°$, C_s symmetry.

1d: *Syn* form, $0° < \Theta_1 < 60°$, $\Theta_2 < 0°$.

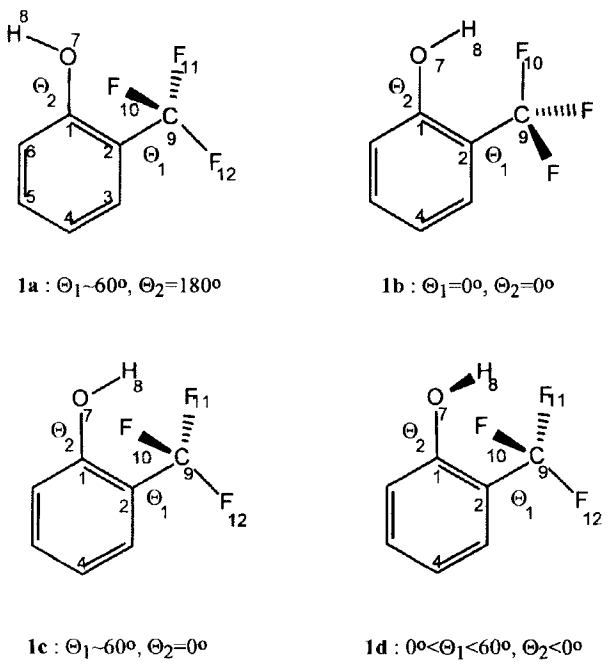

FIGURE 1. Selected conformers of 2-trifluoromethylphenol suggested by spectroscopic and theoretical investigations and the numbering of atoms. Θ_1 is 0° when $F_{10}—C_9—C_2—C_1$ is *syn* and Θ_2 is 0° when $H—O—C_1—C_2$ is *syn*.

Early IR studies[1] proposed the coexistence of two conformers (**1a** and **1b**) based on analogy with the IR spectrum of 2-bromo-6-trifluoromethylphenol. It was concluded that the O—H stretching vibration of the *syn* form, stabilized by intramolecular hydrogen bonding, moved to higher wave numbers compared with the ν_{OH} of the *anti*, non-hydrogen-bonded, form. To our knowledge, this is the only example of such a behavior. Further IR investigations[2,3] supported the original[1] assignment with one exception,[4] which later proved to be incorrect.[5] The energy difference between the **1a** and **1b** forms was determined to be 0.9 kcal/mol, the *syn* being more stable, using temperature-dependent IR measurements.[2]

The existence of intramolecular hydrogen bond in **1** was supported by ^{1}H-NMR and ^{19}F-NMR measurements[6] and by INDO semiempirical quantum chemical calculations with geometry optimization.[7] Both studies suggested a planar six-membered ring for the —C—O—H ··· F—C—C— moiety (**1b**). Another structure was proposed on the basis of microwave spectroscopy,[8] in which the OH hydrogen interacts symmetrically with two fluorine atoms (**1c**). Two prior theoretical investigations, using CNDO/2 and *ab initio* (HF) calculations with the STO-3G basis set, reported contradicting results on the relative conformational stabilities.[5,9]

The inadequacy of the aforementioned computational techniques, their contradictory results, and the importance of these structures have prompted our reinvestigation using more sophisticated meth-

ods. Computational techniques available today for molecules of the complexity of 2-trifluoromethylphenol provide structural information of comparable accuracy to that of the diffraction techniques. Comparison of experimental and computational results mutually enhance their potentials, provided that possible differences in the physical meaning of the parameters originating from different techniques are not ignored.[10] *Ab initio* methods are especially useful in the investigation of series of related compounds for the determination of structural variations, prediction of barriers to internal rotation, and prediction of stabilities of different conformers.[11]

In the present article we report a theoretical analysis of the conformational properties and molecular geometry of **1**. An initial AM1[12] study was performed to predict the low-lying energy conformations on the potential energy hypersurface (PES). At these points, further geometry optimizations were carried out at higher level of theory (HF/6-31G**, MP2/6-31G**). To assess the relative stability of the stationary points of PES, MP2/6-31 + G** energies were evaluated on the MP2/6-31G** geometries, in accordance with the experience, that diffuse functions on the heavy atoms are important for hydrogen binding energetics.[13] The geometrical variations are discussed with reference to the monosubstituted "parent" molecules, viz. phenol (**2**) and trifluoromethylbenzene (**3**), calculated at the same level in the present work.

A further goal of our study was to investigate the reliability of the methods of density functional theory (DFT) for systems like the present one. The main advantage of DFT methods over traditional *ab initio* SCF-MO methods is that they include electron correlation at lower computational cost which is important for larger systems like the one under investigation.

Promising results have been reported in the literature describing hydrogen-bonded systems, O—H ··· O, using DFT methods. Sim and coworkers[14] used DFT to predict structures of comparable quality to those predicted by traditional *ab initio* methods, including electron correlation. A recent study of ethylene glycol by Oie et al.[15] found the DFT results in good agreement with the ones obtained by high level (post-Hartree–Fock) *ab initio* calculations. The potentials of the method for fluorine-containing compounds have been already demonstrated on 1,2-difluoroethane.[16,17] In our comparative study, geometry optimization for special conformers of **1** was performed at four DFT levels, viz. B-LYP, B-P86, B3-LYP, B3-P86 (*vide infra*) with the 6-31G** basis set. The B-P86 theory was used by Sim et al.[14] and was found to give closer agreement with the experimental results than the local spin density approximation parametrized by Vosko, Wilk, and Nussair[18] or the functional of Perdew and Wang.[19,20] The other three methods, introduced recently, gave promising results in the treatment of systems containing heteroatoms.[21-23]

We have also studied the intramolecular hydrogen bonding in the *syn* forms by analysis of the electron density distribution function (ρ). Bader's theory, "atoms in molecules" (AIM),[24] had been applied for the study of hydrogen bonding systems.[25]. This technique locates an atomic interaction line between the participating nuclei of a chemical bond. The electron density maxima at each of the two nuclei are connected by a maximum electron density path, called *bond path*. There is a minimum value of ρ along the path representing also maximum values in directions orthogonal to it. The Hessian matrix of ρ will have two negative and one positive eigenvalues (curvatures) at that point. Hence, the sum of +1 for each positive and −1 for each negative curvature (λ) in ρ is −1 and the point is called the *bond critical point* (*BCP*). Moreover, for a covalent bond the Laplacian of ρ, $\nabla^2\rho$, at the critical point has a negative value, whereas bonds with considerable ionic character have a positive $\nabla^2\rho$ and relatively large ρ at the critical point.[26]

There is also a so-called *ring critical point*, which may be characterized by minimum values of ρ in the plane of the ring, and a maximum with respect to the multifold axis of rotation. The sum of the signs of the curvatures is +1 in this case. Another characteristic bond parameter is the *ellipticity*, by definition $\varepsilon = (\lambda_1/\lambda_2) - 1$, where λ_1 and λ_2 are the first two negative eigenvalues of the Hessian.[27] It describes the symmetry of the electron density distribution along the bond path.

Computational Details

The *ab initio* calculations were performed using 6-31G** double-split-valence plus polarization basis set at the Hartree–Fock (HF), MP2,[28] and different DFT levels. The geometries were fully optimized using gradient optimization routines without any symmetry constraints. The MP2 computations were carried out in the frozen core ap-

proximation. The MP2/6-31 + G** energies were evaluated on MP2/6-31G** geometries.

The following DFT methods were used:

- The B-P86 or Becke–Perdew method, in which Becke's gradient-corrected exchange functional[29] is combined with Perdew's gradient-corrected correlation functional.[20]
- The B-LYP method, in which Becke's gradient-corrected exchange functional[29] is combined with the gradient corrected correlation functional of Lee, Yang, and Parr.[30]
- The B3-P86, which is a linear combination of various exchange and correlation functionals of the form: AE_x[Slater] + $(1 - A)E_x$[HF] + BE_x[Becke] + E_c[VWN] + CE_c[P86], where E_x[Slater], E_x[HF], and E_x[Becke] are the Slater, HF, and Becke exchange functionals (Becke's three-parameter functional), and E_c[VWN] and E_c[P86] are the Vosko, Wilk, and Nussair[18] and the Perdew[20] correlation functionals, respectively. The constants A, B, and C are those determined by Becke by fitting heats of formation ($A = 0.2$, $B = 0.72$, $C = 0.81$).[31]
- The B3-LYP method uses Becke's three-parameter functional with the following correlation functional: CE_c[LYP] + $(1/C) \times E_c$[VWN], where E_c[LYP] is the Lee, Yang, and Parr[30] nonlocal correlation term.

In the DFT calculations the normal grid was used. To obtain the harmonic frequencies the first and second derivatives of the energy with respect to nuclear coordinates were calculated analytically. All the calculations were carried out using the GAUSSIAN 92/DFT[32] computer program on a Silicon Graphics workstation. The properties of the gradient vector field of the electron density were calculated by a modified version of the AIMPAC package[33] from the wave functions provided by the G92/DFT program.

Results and Discussion

HARTREE–FOCK AND MP2 STUDY

A preliminary AM1[12] study was performed to map the PES of **1** as a function of the two rotors, Θ_1(F_{10}—C_9—C_2—C_1) and Θ_2(H—O—C_1—C_2), respectively. The relaxed AM1 PES predicted two energy minima which correspond to structures **1a** and **1c**. Both minima are triply degenerate according to the C_{3v} symmetry of the trifluoromethyl group. The **1b** structure was found to be a saddle-point on the path of the CF_3 rotation between the **1c** conformers. The side-walls of PES are steeper along the Θ_2 axis than along the Θ_1 axis indicating the high energy needed to move the hydrogen out of the plane of the ring, as compared to turning around the trifluoromethyl group. This is consistent with earlier experimental and theoretical results for monosubstituted benzene derivatives.[34, 35]

The geometries corresponding to the AM1 minima were fully optimized using gradient techniques at the HF/6-31G** level. While **1a** emerged as a local minimum also at the HF level, the character of the AM1 *syn* minimum (**1c**) changed. It turned to an energy valley containing two minima of equal energy. In both of them, the hydroxy hydrogen is out of the plane of the benzene ring; Θ_2 is $-14.9°$ and $+14.9°$, respectively; and the dihedral angles F—C_9—C_2—C_1 are $+47.7°$ (F_{10}) and $-47.7°$ (F_{11}), respectively (**1d**). The saddle-point is the symmetric structure **1c** in between, having the O—H hydrogen in the plane of the benzene ring, $\Theta_2 = 0°$, and F_{10} and F_{11} symmetrically positioned to this plane, at $+58.9°$ and $-58.9°$.

Vibrational analysis at the HF/6-31G** level was performed to verify the minimum-energy and saddle-point structures[36] **1a**, **1b**, **1c**, and **1d**. For **1a** and **1d** all the vibrational frequencies proved to be positive, whereas for **1b** and **1c** one frequency appeared imaginary for each, in agreement with the transition-state character of these structures.

To get more reliable data on the geometry and relative stability of the stationary points on the PES of **1** higher level calculations including electron correlation were performed. As the result of the HF treatment the most important geometrical parameters are very similar in magnitude in all the low-energy structures **1a**, **1c**, and **1d**. It is known that the HF level, lacking electron correlation, generally results in too short bonds, especially for those involving highly electronegative elements. Introduction of electron correlation is expected to result in considerable changes.[37] Hence, the geometries obtained at the HF/6-31G** level were further optimized using the same basis set at the MP2 level.[28] Because diffuse functions are known to be important for describing hydrogen binding energetics,[13] single-point MP2/6-31 + G** calculations have been carried out on the MP2/6-31G** geometries. The calculated energies for **1a**, **1b**, **1c**, and **1d** are summarized in Table I.

The computations at the HF and MP2 levels predict a shallow energy valley in the *syn* form **1d**

TABLE I.
Special Forms of Internal Rotation Computed for 1 and Their Energies.

Conformer	Θ_1(°)	Θ_2(°)	Method[a]	E (a.u.)[b]	ΔE (kcal / mol)[c]
1a	60.4	180.0	HF	−641.19186	1.28
			MP2	−642.78869	2.24
			MP2[d]	−642.83450	1.73
			MP2[d] + *ZPVE*[e]	−642.72921	1.83
			B-LYP	−644.35924	2.99
			B-P86	−644.50855	3.04
			B3-LYP	−644.51214	2.55
			B3-P86	−645.97199	2.60
1b	0.0	0.0	HF	−641.19241	0.94
			MP2	−642.79035	1.20
			MP2[d]	−642.83538	1.17
			MP2[d] + *ZPVE*[e]	−642.72983	1.44
1c	58.9	0.0	HF	−641.19361	0.18
			MP2	−642.79175	0.32
			MP2[d]	−642.83721	0.03
			MP2[d] + *ZPVE*[e]	−642.73212	0.00
			B-LYP	−644.36303	0.61
			B-P86	−644.51239	0.63
			B3-LYP	−644.51548	0.45
			B3-P86	−645.97540	0.45
1d	47.7	−14.9	HF	−641.19390	0.00
			MP2	−642.79226	0.00
			MP2[d]	−642.83725	0.00
			MP2[d] + *ZPVE*[e]	−642.73174	0.24
			B-LYP	−644.36401	0.00
			B-P86	−644.51340	0.00
			B3-LYP	−644.51620	0.00
			B3-P86	−645.97612	0.00

[a]The *ab initio* calculations, except where noted, were carried out using 6-31G** basis set.
[b]1 a.u. = 627.5085 kcal / mol.
[c]The difference in the absolute energy relative to the most stable conformer.
[d]MP2 / 6-31 + G** energies calculated on the MP2 / 6-31G** geometry.
[e]Zero-point-vibrational energy (*ZPVE*) corrections were calculated from harmonic vibrational frequencies determined at the HF / 6-31G** level (0.11831 a.u. for **1a**, 0.11860 a.u. for **1b**, 0.11808 a.u. for **1c**, and 0.11855 a.u. for **1d**) and scaled by a factor of 0.89 in accord with known overestimates at this level.[60]

being the global minimum and **1c** a low-lying saddle-point. The largest energy differences between the stationary points of PES were estimated by the MP2/6-31G** level; however, the differences were reduced by the inclusion of diffuse functions on the heavy atoms. The energy difference between **1c** and **1d** was computed to be 0.03 kcal/mol at the MP2/6-31 + G**//MP2/6-31G** level. Corrections for zero-point-vibrational energy (*ZPVE*)[38] to the MP2/6-31 + G**//MP2/6-31G** energy resulted in turning **1c** to be the global minimum[39] and **1d** lying 0.24 kcal/mol above it. At that last level the **1b** saddle-point remained considerably higher in energy than **1d**, by 1.44 kcal/mol. This corresponds to the barrier to internal rotation of the trifluoromethyl group. In this case, the distance between H_8 and F_{10} is the shortest, 1.85 Å (MP2/6-31G**). In accordance with expectations, namely the shortest realistic H···F distance resulting in the most favorable hydrogen bonding, this geometry had been proposed as the most stable in most earlier works.[1-3,6-7] However, the valence electron shell of fluorine is not spherically symmetric due to the definite orientation of the *p* orbitals and, accordingly, the preferred position of the hydrogen relative to the fluorine in a hydrogen bond is not arbitrary. According to the VSEPR model,[40] the most favorable $H_8 \cdots F_{10}$ inter-

action is expected to be in the direction of one of the lone pairs of F_{10}. In case of a planar hexagonal arrangement, H_8 is not found in optimal interaction with any of the fluorine lone pairs. The stabilizing effect of hydrogen bonding is thus considerably diminished in this geometry.

The local minimum character of **1a** was confirmed by all levels under consideration, in agreement with earlier reports.[1-3,5,7-8] The experimentally observed energy difference between the *syn* and *anti* conformers was found to be 0.9 kcal/mol.[2] The HF results are in good agreement with the experimental value, while the MP2 theory predicts double that value. However, the experimental 0.9 kcal/mol is rather tentative because of the poor resolution of the ν_{OH} bands of the *syn* and *anti* forms used for its evaluation.

COMPARISON OF RESULTS OF TRADITIONAL *AB INITIO* AND DFT CALCULATIONS

Data on the performance of DFT methods treating weak interactions are scarce, and we performed a comparative study of the most important conformers of **1** (**1a**, **1c**, **1d**) at different DFT levels (B-LYP, B-P86, B3-LYP, B3-P86) using the G-31G** basis set. The calculated relative stability of the geometry-optimized conformers is presented in Table I. In Table II the average differences in the

TABLE II.
Deviations in Geometrical Data of 1d from the MP2/6-31G Optimized Geometries.[a]**

	HF	B-LYP	B-P86	B3-LYP	B3-P86
r(O—H)	−0.023	0.013	0.014	0.002	0.000
r(C_1—O)	−0.023	0.005	−0.002	−0.008	−0.015
r(C—C)[b]	−0.010	0.012	0.010	0.001	−0.002
r(C_2—C_9)	0.008	0.014	0.011	0.007	0.002
r(C_9—F_{10})	−0.036	0.027	0.020	0.002	−0.005
r(C_9—$F_{11/12}$)	−0.029	0.016	0.010	−0.002	−0.008
r(C—H)[b]	−0.007	0.011	0.013	0.004	0.004
∠H—O—C_1	3.3	−0.7	−1.1	0.4	0.2
∠O—C_1—C_2	−0.2	0.1	0.0	−0.1	−0.2
∠C_1—C_2—C_9	0.6	1.4	1.4	0.9	0.9
∠C—C—C[b]	0.0	0.0	0.0	0.0	0.0
∠H—C—C[b]	0.1	−0.1	−0.2	−0.1	−0.1
∠F_{10}—C_9—C_2	0.3	0.5	0.4	0.3	0.2
∠F_{11}—C_9—C_2	0.3	0.5	0.5	0.3	0.3
∠F_{12}—C_9—C_2	−0.4	0.0	−0.1	−0.1	−0.2
∠F—C_9—F	0.0	−0.4	−0.2	−0.1	−0.1
∠F—C_9—C_2—C_1	−0.3	−9.2	−10.0	−5.6	−6.7
∠H—O—C_1—C_2	−0.9	4.4	4.6	2.4	2.8
∠C—C—C—C[b]	0.0	0.0	0.0	0.0	0.0
∠O—C_1—C_2—C_3	−0.2	−1.1	−1.0	−0.9	−0.9
∠C_9—C_2—C_3—C_4	−1.7	1.1	−1.0	0.3	0.3
∠H—C—C—C[b]	0.2	0.1	0.1	0.1	0.1
∠O—H_8 ··· F_{10}	−4.3	3.3	3.9	1.1	1.5
∠O—H_8 ··· F_{11}	−0.9	2.2	2.8	1.1	1.5
∠H_8 ··· F_{10}—C_9	−0.2	4.4	4.7	2.9	3.5
∠H_8 ··· F_{11}—C_9	1.3	−6.4	−6.9	−3.7	−4.4
d(H_8 ··· F_{10})	0.078	−0.079	−0.104	−0.048	−0.074
d(H_8 ··· F_{11})	0.013	0.211	0.201	0.117	0.118
d(O ··· F_{10})	0.018	−0.04	−0.059	−0.037	−0.061
d(O ··· F_{11})	−0.014	0.24	0.238	0.128	0.133
d(O ··· C_9)	−0.009	0.061	0.051	0.022	0.012

[a]Distances are given in angstroms, angles in degrees. Deviations calculated as the geometrical parameters at MP2/6-31G** are subtracted from the ones obtained at HF/6-31G** or DFT/6-31G**.
[b]Average deviation of the ring geometrical parameters.

geometrical parameters with respect to the MP2/6-31G** results are shown for **1d**. They are similar to those obtained for **1a** and **1c**. A list of individual parameters for all three structures is available from the authors upon request.

The data in Table I show that inclusion of electron correlation in the computations at the respective DFT levels does not change the **1d** structure being energetically the most favorable, and **1a** being the least. There are, however, changes in the energy differences between the conformers. The DFT calculations estimate larger stability of **1d** with respect to **1a** and **1c** than the HF and MP2 levels do.

A systematic variation in bond lengths can be observed for all conformers. The HF level with a good quality basis set is known to underestimate the bond lengths because of the improper treatment of electron correlation.[21,41] In our study, the bonds resulting from the HF calculations are consistently shorter, with the exception of the C_2—C_9 bond, than the corresponding MP2 ones (Table II): the differences are between 0.007 and 0.036 Å. The differences of $r(C_9—F_{10})$ and $r(C_9—F_{11})$ from the MP2 values vary for **1d** because of the asymmetrical arrangement of the two *syn* fluorines.

At the B-LYP and B-P86 levels the bonds are generally longer than the MP2 ones by about 0.01 Å. This trend is not followed by r(C—F) at B-LYP and by r(C—O) at B-P86. At the B3-LYP level the bond lengths are in good agreement with those calculated at the MP2/6-31G** level with a maximum difference of 0.008 Å. Here, $r(C_1—O)$ is consistently underestimated while $r(C_2—C_9)$ is overestimated. Somewhat poorer agreement was achieved with the B3-P86 calculations. Each method is sensitive to the nonequivalent environments of F_{10} and F_{11} in **1d**.

Most, though not all, bond angles calculated at both the HF and DFT levels are in good agreement with those calculated at the MP2/6-31G** level. In general the B3-LYP and B3-P86 levels yield the closest values to the results of the MP2 method.

The torsional angles calculated at different levels are also in good agreement. Exceptions are the F—C—C—C and H—O—C—C torsions in **1d**, where the DFT values differ considerably from those of the HF and post-HF calculations. The DFT methods rotate the trifluoromethyl group more, and the hydroxy group less from the symmetrical position found in **1c**. This effect seems consistent with DFT predicting shorter $H_8 \cdots F_{10}$ and $O \cdots F_{10}$ distances in **1d** (Table II) and with the increased stability of **1d** with respect to **1a** (Table I) as compared with the results at the MP2 level. Thus, the DFT methods may overestimate the interaction between H_8 and F_{10} with respect to the HF and post-HF levels.

Experimental rotational constants of **1** have been reported,[8] and they are shown in Table III together with the computed ones for all three conformers. Differences in the measured and computed rotational constants, say, within 1%, or even more, may be attributed to the difference in the physical meaning of these parameters. Considering this, the rotational constants calculated at the MP2, B3-LYP, and B3-P86 levels are in excellent agreement with the experimental values. Thus, these three methods seem to be well suited for describing the geometry of such compounds. It is also observed that the three conformers **1a**, **1c**, and **1d** cannot be

TABLE III.
Rotational Constants (Megahertz) for 1a, 1c, and 1d Conformers.[a]

		HF	MP2	B-LYP	B-P86	B3-LYP	B3-P86	Expt.[b]
1a	A	1963.4	1914.4	1872.8	1883.5	1910.8	1924.2	
	B	948.9	940.5	918.1	922.9	934.0	940.6	
	C	717.9	710.6	694.0	697.5	706.0	710.8	
1c	A	1956.3	1906.0	1869.7	1882.3	1907.3	1922.1	1916.349 ± 0.091
	B	950.8	942.7	921.2	926.5	936.8	944.0	939.1730 ± 0.0097
	C	717.2	709.9	694.8	698.7	706.4	711.7	708.745 ± 0.014
1d	A	1950.0	1899.2	1856.6	1867.7	1897.3	1910.5	
	B	949.1	940.6	916.8	922.2	933.8	940.3	
	C	715.9	708.4	691.1	695.0	704.0	708.7	

[a] Geometries are optimized using 6-31G** basis set.
[b] Rotational constants from microwave spectroscopy.[8] They were attributed to conformer **1c**.

distinguished on the basis of the rotational constants alone.

GEOMETRY OF PHENOL AND TRIFLUOROMETHYLBENZENE

To evaluate the structural variations induced by ortho substitution and, in particular, to investigate the geometrical consequences of intramolecular hydrogen bonding in the rest of the molecule, geometry optimization of the "parent" molecules, viz. phenol (**2**) and trifluoromethylbenzene (**3**), was carried out at the MP2/6-31G** level.[42]

Before turning to the geometrical parameters a caveat should be issued at this point; an absolute agreement of computed bond lengths with the experimental ones should not be sought because of their different physical meaning.[10] As a general rule, the computed equilibrium bond length should be smaller than the corresponding average bond length determined by any experiment, the latter also depending on the particular technique used.[10,43] Parameter *differences*, of course, are much less influenced by these indeterminacies than their absolute values.

Results from selected studies on the geometry of phenol are given in Table IV. The asymmetric attachment of the OH substituent causes deviation from axial symmetry in the ring geometry. Experimental[44,45] and *ab initio* MO studies[46-49] have consistently indicated that these deviations are small, a few thousands of an angstrom in the bond lengths and a few tenths of a degree in the angles. Because these small differences are within experimental error, the microwave and computational geometrical parameters of the benzene ring have been averaged to be consistent with C_{2v} symmetry of the ring in the electron diffraction analysis.[45]

Detailed comparison of the absolute values of the electron diffraction and *ab initio* parameters would not be meaningful because of their different physical meaning. The computed data refer to the equilibrium geometry (r_e). On the other hand, the parameters from gas-phase electron diffraction incorporate all vibrational effects at the temperature of the experiment[50] and the resulting average bond lengths, r_g, should always be greater than the calculated r_e ones. For a relatively rigid system like the benzene ring, differences of 0.004–0.008 Å are reasonable between r_g and r_e. Better agreement can be expected between r_e and the r_s effective internuclear distance from microwave spectroscopy based on complete isotopic substitution. Although the r_s structure does not have a rigor-

TABLE IV.
Molecular Geometry of Phenol[a]

Parameter	Electron diffraction[b]	Microwave spectroscopy[c,d]	*Ab initio* MO calculations[d] HF / 6-31G*[e]	MP2(FC) / 6-31G**[f]	MP2(FULL) / 6-31G*[g]
$r(C_1—C_2)$		1.391 ± 0.005	1.387	1.397	1.396
$r(C_2—C_3)$	1.399 ± 0.003	1.393 ± 0.005	1.384	1.395	1.393
$r(C_3—C_4)$		1.395 ± 0.004	1.386	1.396	1.395
$r(C_1—O_7)$	1.381 ± 0.004	1.375 ± 0.005	1.353	1.374	1.374
$r(C—H)_{mean}$	1.086 ± 0.003	1.083 ± 0.003	1.075	1.083	1.087
$r(O—H)$	0.958 ± 0.003	0.957 ± 0.006	0.947	0.965	0.973
$\angle C_2—C_1—C_6$	121.6 ± 0.2	120.9 ± 0.4	120.2	120.3	120.3
$\angle C_1—C_2—C_3$	118.8 ± 0.2	119.3 ± 0.3	119.6	119.6	119.6
$\angle C_2—C_3—C_4$	120.6 ± 0.5	120.6 ± 0.3	120.7	120.6	120.5
$\angle C_3—C_4—C_5$	119.7 ± 0.8	119.2 ± 0.2	119.2	119.4	119.4
$\angle C_2—C_1—O_7$	121.2 ± 1.2	122.1 ± 0.3	122.4	122.8	122.8
$\angle C—O—H$	106.4 ± 3.7	108.8 ± 0.4	110.7	108.4	108.4

[a] Bond distances are given in angstroms, angles in degrees.
[b] Ref. 45, bond distances are r_g values.
[c] Ref. 44, r_s structure.
[d] Mean values of geometrical parameters are given to be consistent with C_{2v} symmetry.
[e] Ref. 48.
[f] This study.
[g] Ref. 49.

ously defined physical meaning, it is very close to r_e for any practical purpose.[43] A complete r_s structure has been published for phenol.[44] As expected, the MP2 data are in good agreement with the r_s values, if considering experimental error, except for the O—H bond length, which is slightly overestimated. Altogether, the performance of the post-HF method is better than that of the HF computations.

For trifluoromethylbenzene, the stable form was reported to have one of the C—F bonds perpendicular to the benzene ring by STO-3G MO computations.[51] Our calculations confirmed this result. They also found the benzene ring bond lengths to be hardly effected by substitution, in agreement with an earlier electron diffraction investigation[34] (see Table V). The pattern of the computed ring angles is closer to the expectations[52] than the experimental ones, considering the electronegativity of the substituents, and adopting the additivity of substituent effects, although the deviations are small in any case. The MP2 computations overestimate the C—F bond length, and some of the HF-calculated bond lengths appear to be too small, as is often the case.

Characteristic computed distances and angles of **1a**, **1c**, **1d**, **2**, and **3** at the MP2/6-31G** level are compiled in Table VI. They will be discussed in the next subsection.

DISCUSSION OF STRUCTURE AND HYDROGEN BONDING

The most interesting structural question of the title molecule is the formation of intramolecular hydrogen bond and its relationship to the geometrical changes in the rest of the molecule. By geometrical changes we mean the differences as compared to the "parent" molecules, viz. phenol and trifluoromethylbenzene. The basis of this discussion is the results of the MP2/6-31G** calculations. Figure 2a and b summarizes the bond lengths and bond angles, respectively, under consideration.

The C—F bond, whose fluorine is involved in the hydrogen bonding, is markedly longer than the C—F bond of $C_6H_5CF_3$ and the C—F bond *anti* to the hydrogen bond shortens as compared with $C_6H_5CF_3$. The differences among the three C—F bond lengths of 2-trifluoromethylphenol appear to be very characteristic. The longest bond leads to the most involved fluorine and the shortest to the least involved one. There is a shortening of the C—O bond and of the C—CF_3 bond, as compared with those of phenol and trifluoromethylbenzene, respectively. Some of the bond length changes are marginal, however, all of them are consistent with Scheme 1 describing the title molecule in terms of resonance structures. This is especially well expressed by the lengthening of the C_1—C_2 bond

TABLE V.
Molecular Geometry of Trifluoromethylbenzene.[a]

Parameter	Electron diffraction[b]	*Ab initio* MO calculations[c]	
		HF / 6-31G**	MP2(FC) / 6-31G**
$r(C—C)^d_{ring}$	1.397 ± 0.003	1.385	1.396
$r(C_2—C_9)$	1.504 ± 0.004	1.503	1.496
$r(C_9—F)^d$	1.345 ± 0.003	1.325	1.355
$r(C—H)^d$	1.099 ± 0.005	1.075	1.082
$\angle C_1—C_2—C_3$	119.7 ± 0.3	120.3	120.8
$\angle C_2—C_3—C_4$	120.4 ± 0.3	119.8	119.4
$\angle C_3—C_4—C_5$	119.4 ± 0.3	120.0	120.2
$\angle C_4—C_5—C_6$	120.7 ± 0.4	120.1	120.0
$\angle C_2—C_9—F^d$	111.9 ± 0.1	111.9	111.8
$\angle F—C_9—F^d$	106.9 ± 0.1	106.9	107.0

[a] Bond distances are given in angstroms, angles in degrees; the numbering of atoms is consistent with that of 2-trifluoromethylphenol (see Fig. 1).
[b] Ref. 34, bond distances are r_g values.
[c] This study.
[d] Mean value.

TABLE VI.
Structural Parameters[a] of Phenol (2), Trifluoromethylbenzene (3), and Conformers of 2-Trifluoromethylphenol (1a, 1c, 1d) Calculated at MP2 / 6-31G Level.**

	2	3	1a	1c	1d
$r(O—H)$	0.965	—	0.966	0.966	0.966
$r(C_1—O)$	1.374	—	1.367	1.366	1.367
$r(C_1—C_2)$	1.397	1.397	1.404	1.405	1.405
$r(C_2—C_3)$	1.396	1.397	1.395	1.398	1.399
$r(C_3—C_4)$	1.395	1.394	1.395	1.391	1.391
$r(C_4—C_5)$	1.398	1.396	1.394	1.398	1.397
$r(C_5—C_6)$	1.393	1.396	1.395	1.391	1.391
$r(C_6—C_1)$	1.398	1.394	1.396	1.397	1.398
$r(C_2—C_9)$	—	1.496	1.498	1.491	1.492
$r(C_9—F_{10})$	—	1.354	1.351	1.363	1.374
$r(C_9—F_{11})$	—	1.355	1.351	1.363	1.354
$r(C_9—F_{12})$	—	1.354	1.356	1.345	1.346
$r(C_1—H)$	—	1.081	—	—	—
$r(C_2—H)$	1.085	—	—	—	—
$r(C_3—H)$	1.083	1.081	1.080	1.081	1.081
$r(C_4—H)$	1.082	1.082	1.081	1.081	1.081
$r(C_5—H)$	1.083	1.082	1.082	1.082	1.082
$r(C_6—H)$	1.082	1.082	1.084	1.082	1.082
$\angle H—O—C_1$	108.4	—	108.6	110.4	109.5
$\angle O—C_1—C_2$	122.8	—	117.5	124.4	124.2
$\angle C_1—C_2—C_9$	—	119.6	119.5	119.0	119.9
$\angle C_6—C_1—C_2$	120.3	119.4	119.6	119.2	119.2
$\angle C_1—C_2—C_3$	119.7	120.8	119.8	120.2	120.1
$\angle C_2—C_3—C_4$	120.5	119.4	120.5	120.2	120.3
$\angle C_3—C_4—C_5$	119.4	120.2	119.6	119.5	119.5
$\angle C_4—C_5—C_6$	120.6	120.0	120.3	120.6	120.5
$\angle C_5—C_6—C_1$	119.6	120.2	120.2	120.2	120.3
$\angle H—C_1—C_2$	—	119.9	—	—	—
$\angle H—C_2—C_1$	120.0	—	—	—	—
$\angle H—C_3—C_2$	119.3	119.9	119.0	119.0	119.0
$\angle H—C_4—C_5$	120.3	120.1	120.4	120.5	120.5
$\angle H—C_5—C_6$	119.3	120.0	119.4	119.3	119.4
$\angle H—C_6—C_1$	118.8	119.8	119.5	118.1	118.2
$\angle F_{10}—C_9—C_2$	—	111.9	111.9	111.4	111.4
$\angle F_{11}—C_9—C_2$	—	111.6	111.9	111.4	112.1
$\angle F_{12}—C_9—C_2$	—	111.9	111.4	113.4	113.0
$\angle F_{10}—C_9—F_{11}$	—	106.9	107.4	105.4	105.7
$\angle F_{10}—C_9—F_{12}$	—	107.4	106.9[b]	107.5	106.7
$\angle F_{11}—C_9—F_{12}$	—	106.9	107.0[b]	107.5	107.5
$\angle F_{10}—C_9—C_2—C_1$	—	31.7	60.3	58.6	48.0
$\angle F_{11}—C_9—C_2—C_1$	—	−88.0	−60.3	−58.6	−70.1
$\angle F_{12}—C_9—C_2—C_1$	—	152.3	180.0	180.0	168.2
$\angle H—O—C_1—C_2$	0.1	—	180.0	0.0	−14.0
$\angle C_1—C_2—C_3—C_4$	0.0	−0.5	0.0	0.0	−0.4
$\angle C_2—C_3—C_4—C_5$	0.0	0.4	0.0	0.0	0.8
$\angle C_3—C_4—C_5—C_6$	0.0	−0.3	0.0	0.0	−0.9
$\angle C_4—C_5—C_6—C_1$	0.0	0.3	0.0	0.0	0.7
$\angle C_5—C_6—C_1—C_2$	0.0	−0.3	0.0	0.0	−0.3
$\angle C_6—C_1—C_2—C_3$	0.0	0.5	0.0	0.0	0.2
$\angle O—C_1—C_2—C_3$	0.0	—	180.0	180.0	−179.4
$\angle C_9—C_2—C_3—C_4$	—	−176.9	179.9[b]	180.0	−175.6
$\angle H—C_1—C_2—C_3$	—	179.7	—	—	—

(Continues on next page)

TABLE VI.
(Continued)

	2	3	1a	1c	1d
$\angle H-C_2-C_1-C_6$	180.0	—	—	—	—
$\angle H-C_3-C_2-C_1$	180.0	180.3	180.0	180.0	179.9
$\angle H-C_4-C_5-C_6$	180.0	179.7	180.0	180.0	179.6
$\angle H-C_5-C_6-C_1$	180.0	179.9	180.0	180.0	179.9
$\angle H-C_6-C_1-C_2$	180.0	179.6	180.0	180.0	179.7
$\angle O-H_8\cdots F_{10}$	—	—	—	123.9	137.1
$\angle O-H_8\cdots F_{11}$	—	—	—	123.9	108.9
$\angle H_8\cdots F_{10}-C_9$	—	—	73.6	78.8	92.6
$\angle H_8\cdots F_{11}-C_9$	—	—	73.6	78.8	64.2
$d(H_8\cdots F_{10})$	—	—	3.736	2.285	1.983
$d(H_8\cdots F_{11})$	—	—	3.736	2.285	2.731
$d(O\cdots F_{10})$	—	—	2.836[b]	2.935	2.771
$d(O\cdots F_{11})$	—	—	2.835[b]	2.935	3.179
$d(O\cdots C_9)$	—	—	2.775	2.905	2.922

[a]Distances in angstroms, angles in degrees; for numbering of atoms see Figure 1.
[b]The small deviation from the C_s symmetry is due to the 0.01 gradient change (standard) limit and that no symmetry constraint was used in the optimization procedure.

and the shortening of the C_3—C_4 and C_5—C_6 bonds. Overall, the structure of 2-trifluoromethylphenol may be characterized by resonance-assisted hydrogen bonding.[53]

Considering the bond angles, the tilt of the C—O bond is more pronounced in the title molecule than in phenol, and the C—O—H angle increases. The changes are much smaller in the part of the molecule containing the trifluoromethyl group. Here the C—CF_3 bond remains untilted and the C—C—F bond angle involved in the hydrogen bonding decreases slightly which is consistent with the weakened C—F bond (cf. the VSEPR model[40]) and with accommodating the F···H interaction.

The F···H hydrogen bond is 1.98 Å in length which corresponds to medium-strength interaction. It is comparable to the hydrogen bond in tetrafluorohydroquinone,[54] 2.02 ± 0.07 Å, in which the geometrical consequences of hydrogen bond formation in the rest of the molecule are also comparable to the present findings. Even very weak attractive interactions that would hardly qualify for a hydrogen bond, such as H···O of 2.4 Å in *N,N*-dimethylformamide[55] and 2.30 Å in dimethylcarbamyl chloride,[56] have been observed to have appreciable consequences in the structure of the rest of the molecule.

The variation of the geometrical parameters is closely related to the changes of the electron density distribution (ρ). This distribution, in itself, is a sensitive measure of the bonding interactions. The ρ of **1d** and **1c** was calculated from the MP2/6-31G** wave functions. The bond parameters determined from the electron density distribution of **1d** and **1c** are shown in Tables VII and VIII, respectively. The bond properties of C_4—H, C_5—H and C_6—H are very similar to the ones of C_3—H, and only the latter is presented in the tables. Because of the C_s symmetry of **1c**, C_9—F_{10} is identical to C_9—F_{11}.

The bond properties of **1c** and **1d** show characteristic features of the compound. An alternation in the bond distances C_2—C_3, C_3—C_4, C_4—C_5, and C_5—C_6 can be observed, which is reflected in the larger electron density and negative Laplacian values at the *bond critical points* (*BCPs*) of the shorter bonds and the smaller ρ and lower magnitude of the negative $\nabla^2\rho$ of the longer ones. The ρ and $\nabla^2\rho$ of *BCP* of C_6—C_1 and C_1—C_2 deviate somewhat in magnitude from the trend of the aforementioned bonds. This may be the result of hyperconjugation of the lone pair of O_7 with the aromatic π-system. The electron density distribution of these two bonds is also more elliptic than the one of the less affected bonds.

Due to the large electronegativity of F the *BCPs* of the C—F bonds are not at the middle of the distance between the two atoms, but closer to the respective carbons. The longer C—F bonds have smaller electron density at the *BCP* and, as the λ_3 values show, more flat electron density function around it. This effect is dominant, thus the Laplacian of ρ decreases with the bond lengthening at

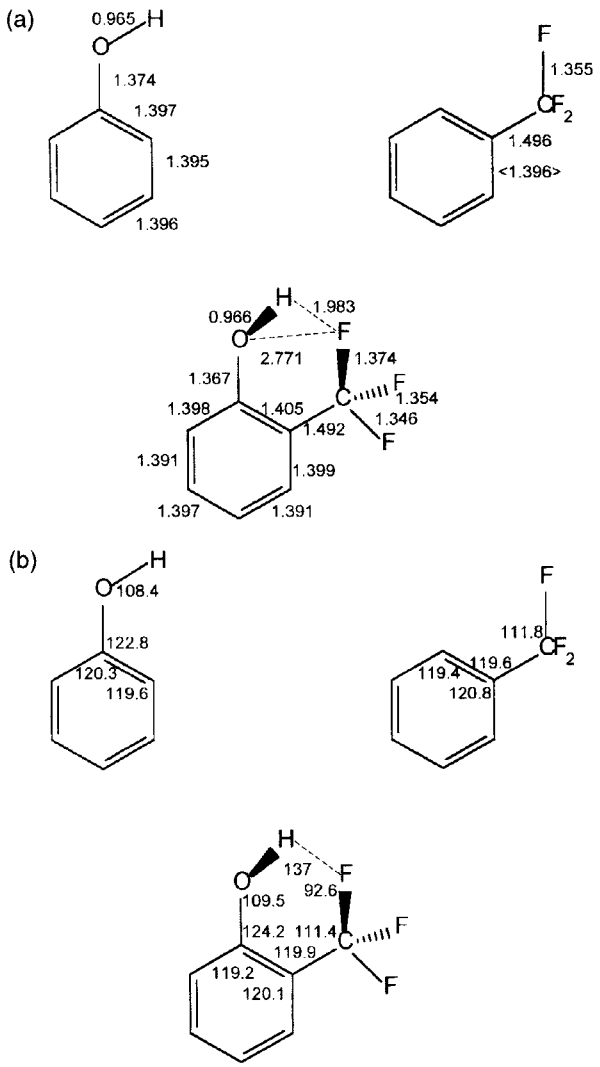

FIGURE 2. Comparison of important geometrical parameters of 2-trifluoromethylphenol with those of phenol and trifluoromethylbenzene: (a) bond lengths (angstroms); (b) bond angles (degrees).

the given range. The *ellipticity* of the longer C—F bonds is also slightly more pronounced. We call the attention to the negative sign of $\nabla^2\rho$ at the *BCP* of the C—F bonds. This shows, that at the MP2 level, the C—F bonding involves less ionic character than suggested earlier on the basis of positive $\nabla^2\rho$ obtained at the HF level.[57,58]

The interaction between the hydroxy and trifluoromethyl groups results in smaller ρ but larger magnitude of the negative $\nabla^2\rho$ and ε at the *BCP*s of the C_9—F_{10} and C_9—F_{11} bonds. The effect is the largest for C_9–F_{10} in **1d**, where the strongest interaction was found (cf. the C—F bond lengthening). Other (weaker) interactions between H_8 and F_{11} in **1d**, and H_8 and $F_{10/11}$ in **1c** are reflected in the intermediate bond parameter values of the respective C—F bonds in between those of C_9—F_{10} and C_9—F_{12} in **1d**.

Beside the normal covalent bonds, a *bond critical point*, in Bader's sense,[24] was found between H_8 and F_{10} in **1d**, providing graphic evidence for hydrogen bonding interaction. The positions of the *critical points* with respect to the atomic nuclei are shown in Figure 3. The ρ and $\nabla^2\rho$ values at this *BCP* are in the ranges observed earlier for hydrogen bonds, i.e., 0.002–0.035 a.u. for ρ and 0.024–0.139 a.u. for $\nabla^2\rho$, respectively.[25] In addition, two *ring critical points* are observed, one for the aromatic ring and another one for the hydrogen bonded six-ring structure. The bent character of the $H_8 \cdots F_{10}$ hydrogen bond can be seen from the sum of the nuclear distances to the *BCP*, which is 0.008 Å larger than the calculated $H_8 \cdots F_{10}$ internuclear distance at the same level of theory (cf. Tables VI and VII). The variations of all the bond distances, $r(A) + r(B)$, in Table VII are consistent with the calculated internuclear distances in the molecule.

Analysis of ρ of **1c** indicates that no *bond critical points* were found between H_8 and the respective fluorines, and also no *ring critical points* are present inside of the —C—O—H $\cdots$ $F_{10/11}$—

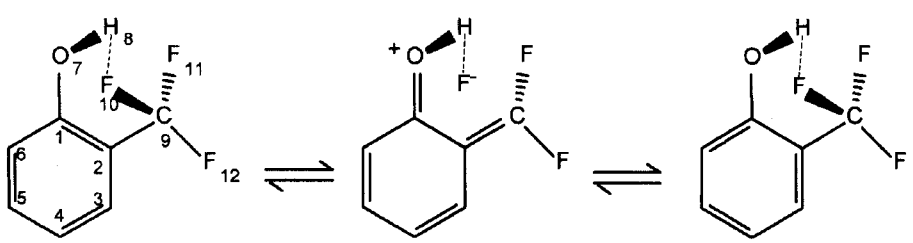

SCHEME 1.

TABLE VII.
Bond Properties[a] of 1d Based on MP2 / 6-31G Wave Function.**

A	B	r(A)	r(B)	r(A) + r(B)	ρ	$\nabla^2\rho$	ε	λ_1	λ_2	λ_3	Type[b]
C_6	C_1	0.672	0.726	1.398	0.3140	−0.8837	0.2487	−0.6693	−0.5360	0.3216	−1
C_1	C_2	0.714	0.692	1.406	0.3060	−0.8173	0.2640	−0.6415	−0.5076	0.3318	−1
C_2	C_3	0.715	0.684	1.399	0.3049	−0.8090	0.2307	−0.6234	−0.5065	0.3209	−1
C_3	C_4	0.702	0.689	1.391	0.3122	−0.8550	0.2293	−0.6485	−0.5276	0.3211	−1
C_4	C_5	0.697	0.700	1.397	0.3093	−0.8438	0.2158	−0.6410	−0.5272	0.3244	−1
C_5	C_6	0.691	0.700	1.391	0.3116	−0.8509	0.2306	−0.6461	−0.5250	0.3202	−1
C_1	O_7	0.453	0.914	1.367	0.2858	−0.3790	0.0218	−0.5823	−0.5698	0.7731	−1
H_8	O_7	0.187	0.779	0.966	0.3611	−2.0997	0.0237	−1.8546	−1.8117	1.5666	−1
C_2	C_9	0.688	0.804	1.492	0.2782	−0.7647	0.0517	−0.5685	−0.5406	0.3444	−1
C_9	F_{10}	0.461	0.913	1.374	0.2562	−0.2950	0.1512	−0.5638	−0.4897	0.7585	−1
C_9	F_{11}	0.452	0.902	1.354	0.2703	−0.2777	0.1384	−0.6230	−0.5472	0.8925	−1
C_9	F_{12}	0.446	0.900	1.346	0.2732	−0.2183	0.1391	−0.6413	−0.5630	0.9860	−1
H	C_3	0.399	0.682	1.081	0.2879	−1.0661	0.0186	−0.7682	−0.7542	0.4563	−1
H_8	F_{10}	0.750	1.241	1.991	0.0220	0.0799	0.0415	−0.0292	−0.0281	0.1372	−1
C_2	C_6	1.387	1.391	2.778	0.0204	0.1589	0.0000	−0.0147	0.0825	0.0911	+1
H_8	F_{10}	1.065	1.411	2.476	0.0137	0.0854	0.0000	−0.0099	0.0347	0.0606	+1

[a] r(A) and r(B) are the distances from the nuclei A and B, respectively, to the *bond* (or *ring*) *critical point* in angstroms; ρ is the charge density (e / a.u.^{3}) at the critical point; $\nabla^2\rho$ is the Laplacian of ρ at the critical point; ε is the *bond ellipticity*; and the λ values are the curvatures of ρ at the critical point.
[b] The sum of +1 for each positive and −1 for each negative curvature (λ) in ρ: −1 indicates a *bond critcal point*, whereas +1 indicates a *ring critical point*, respectively.

C—C— moieties. This implies that no hydrogen bonding interaction occurs in **1c**. However, the properties of the H_8—O_7, C_9—F_{10}, and C_9—F_{11} bonds (including the C—F bond distances) show an electrostatic attractive interaction between H_8 and the fluorines also in this conformer, although to lesser extent than in the case of H_8 and F_{10} in **1d**. It should be noted that it is rather difficult to observe *critical points* of weak interactions, because they appear as a weak minimum in a slightly

TABLE VIII.
Bond Properties[a] of 1c Based on MP2 / 6-31G Wave Function.**

A	B	r(A)	r(B)	r(A) + r(B)	ρ	$\nabla^2\rho$	ε	λ_1	λ_2	λ_3	Type[b]
C_6	C_1	0.671	0.727	1.398	0.3140	−0.8842	0.2486	−0.6691	−0.5359	0.3208	−1
C_1	C_2	0.715	0.691	1.406	0.3064	−0.8198	0.2626	−0.6423	−0.5087	0.3311	−1
C_2	C_3	0.715	0.683	1.398	0.3052	−0.8106	0.2320	−0.6243	−0.5067	0.3205	−1
C_3	C_4	0.703	0.689	1.392	0.3120	−0.8542	0.2292	−0.6482	−0.5273	0.3213	−1
C_4	C_5	0.697	0.701	1.398	0.3092	−0.8431	0.2164	−0.6408	−0.5268	0.3244	−1
C_5	C_6	0.691	0.700	1.391	0.3114	−0.8500	0.2313	−0.6457	−0.5244	0.3201	−1
C_1	O_7	0.452	0.915	1.367	0.2851	−0.3568	0.0079	−0.5753	−0.5708	0.7892	−1
H_8	O_7	0.189	0.777	0.966	0.3622	−2.0926	0.0232	−1.8463	−1.8045	1.5582	−1
C_2	C_9	0.688	0.803	1.491	0.2788	−0.7676	0.0524	−0.5705	−0.5421	0.3449	−1
C_9	F_{10}	0.456	0.907	1.363	0.2637	−0.2899	0.1444	−0.5940	−0.5190	0.8231	−1
C_9	F_{12}	0.446	0.899	1.345	0.2735	−0.2086	0.1386	−0.6432	−0.5649	0.9995	−1
H	C_3	0.399	0.682	1.081	0.2879	−1.0668	0.0186	−0.7686	−0.7545	0.4563	−1
C_2	C_6	1.386	1.391	2.777	0.0204	0.1590	0.0000	−0.0147	0.0826	0.0911	+1

[a] r(A) and r(B) are the distances from the nuclei A and B, respectively, to the *bond* (or *ring*) *critical point* in angstroms; ρ is the charge density (e / a.u.^{3}) at the critical point; $\nabla^2\rho$ is the Laplacian of ρ at the critical point; ε is the *bond ellipticity*; and the λ values are the curvatures of ρ at the critical point.
[b] The sum of +1 for each positive and −1 for each negative curvature (λ) in ρ: −1 indicates a *bond critical point* whereas, +1 indicates a *ring critcal point*, respectively.

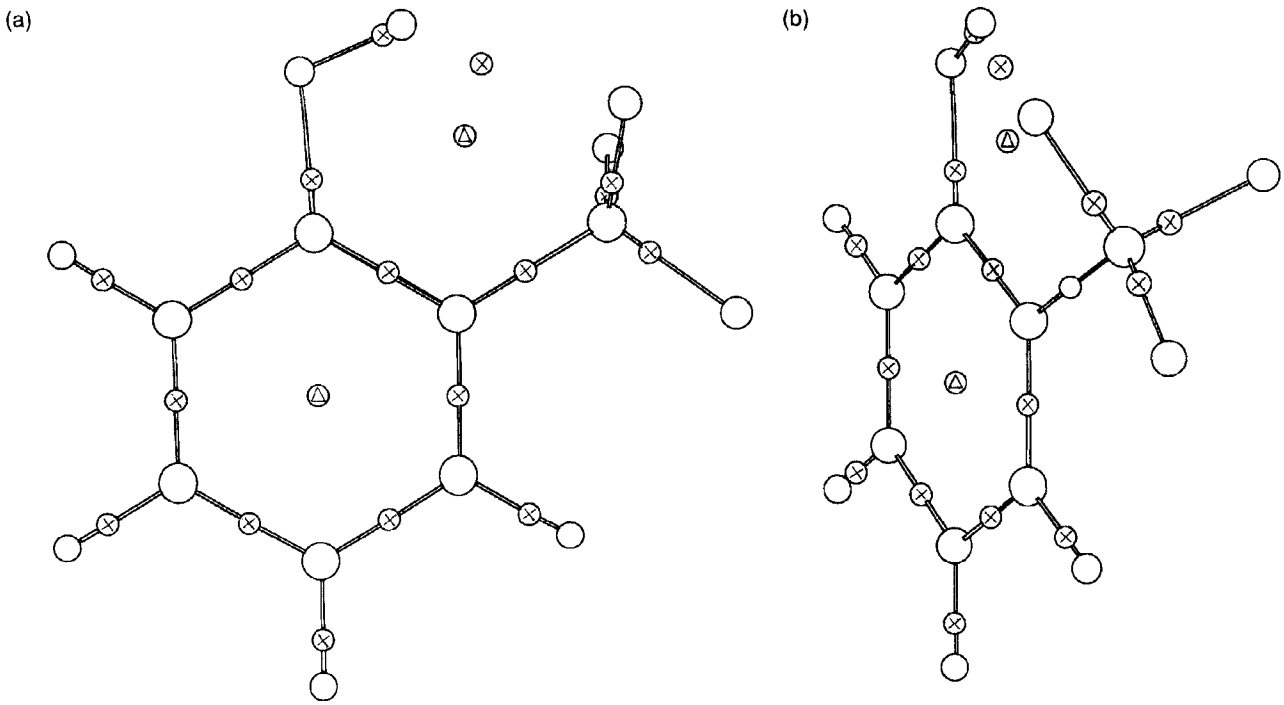

FIGURE 3. The positions of *bond* (x) and *ring* (Δ) *critical points* with respect to the atomic nuclei (from two directions) in **1d**.

varying, low-density electron gas. Under these circumstances, the location of a minimum is difficult to find with the usual algorithm and precision.[25,59]

Conclusions

1. The global minimum of the MP2/6-31G** potential energy hypersurface of 2-trifluoromethylphenol corresponds to a structure in which the O—H bond points toward the trifluoromethyl group and there is a 1.98-Å-long hydrogen bond to one of the fluorines. The O—H bond is slightly rotated, whereas the C—F bond, involved in the hydrogen bond, is considerably rotated from the plane of the benzene ring, both pointing to the same side of the ring. The symmetrical form in which the O—H bond is in the plane and the two C—F bonds are at 59° of torsion, is a saddle-point. At the MP2/6-31 + G**//MP2/6-31G** + *ZPVE* level this saddle-point turns out to be the global minimum. There is a second minimum, higher in energy by about 2 kcal/mol than the global minimum, in which the O—H bond points away from the trifluoromethyl group.
2. The formation of the intramolecular hydrogen bond is also pronounced in the appearance of a *bond critical point* in Bader's sense. This is in the space between the hydrogen and fluorine atoms involved in hydrogen bonding.
3. All geometrical changes in the rest of the molecule, as compared with phenol and trifluoromethylbenzene, are consistent with resonance-assisted hydrogen bonding.
4. The structure computed for 2-trifluoromethylphenol is in excellent agreement with experimentally determined rotational constants[8] which, however, do not appear to be conformation-specific enough to aid in the conformational analysis of this molecule.
5. Two (B3-LYP and B3-P86) of the four DFT methods tested provided calculated geometries in excellent agreement with those of the MP2 calculations.

Acknowledgments

We are grateful to Dr. V. Izvekov for helpful comments and suggestions. This research has been supported by the Hungarian Scientific Research Foundation (OTKA, Nos. T014247 and T014945).

This workstation used in this investigation was acquired with the assistance of the Hungarian State Committee for Technical Development (OMFB) and the J. Varga Foundation of the Budapest TechnicalUniversity.

References

1. A. W. Baker and A. T. Shulgin, *Nature*, **206**, 712 (1965).
2. E. V. Konovalov, Yu. P. Egorov, R. V. Belinskaya, V. N. Boiko, and L. M. Yagupol'skii, *Zh. Prikl. Spektrosk.*, **14**, 484 (1971); *Chem. Abstr.*, **75**, 42673a (1971).
3. T. N. Pliev, *Izv. Vyssh. Uchebn. Zaved., Khim. Khim. Tekhnol.*, **30**, 29 (1986); *Chem. Abstr.*, **108**, 93972e (1988).
4. F. C. Marler, III and H. P. Hopkins, Jr., *J. Phys. Chem.*, **74**, 4164 (1970).
5. S. W. Dietrich, E. C. Jorgensen, P. A. Kollman, and S. Rothenberg, *J. Am. Chem. Soc.*, **98**, 8310 (1976).
6. D. Doddrell, E. Wenkert, and P. V. Demarco, *J. Mol. Spectrosc.*, **32**, 162 (1969).
7. E. Canadell, J. Catalan, and J. I. Fernandez-Alonso, *Adv. Mol. Relax. Interact. Proc.*, **12**, 265 (1978).
8. K.-V. Hansen and T. Pedersen, *J. Mol. Struct.*, **97**, 311 (1983).
9. T. Silvestro and R. D. Topsom, *J. Mol. Struct. (Theochem)*, **206**, 309 (1990).
10. M. Hargittai and I. Hargittai, *Int. J. Quantum Chem.*, **44**, 1057 (1992).
11. J. R. Durig and A. Wang, *J. Mol. Struct.*, **294**, 13 (1993).
12. M. J. S. Dewar, E. G. Zoebisch, E. F. Healy, and J. J. P. Stewart, *J. Am. Chem. Soc.*, **107**, 3902 (1985).
13. J. E. Del Bene, W. B. Person, and K. Szczepaniak, *J. Phys. Chem.*, **99**, 10705 (1995).
14. F. Sim, A. St.-Amant, I. Papai, and D. R. Salahub, *J. Am. Chem. Soc.*, **114**, 4391 (1992).
15. T. Oie, I. A. Topol, and S. K. Burt, *J. Phys. Chem.*, **98**, 1121 (1994).
16. D. A. Dixon, N. Matsuzawa, and S. C. Walker, *J. Phys. Chem.*, **96**, 10740 (1992).
17. I. A. Topol and S. K. Burt, *Chem. Phys. Lett.*, **204**, 611 (1993).
18. S. H. Vosko, L. Wilk, and M. Nussair, *Can. J. Phys.*, **58**, 1200 (1980).
19. J. P. Perdew and Y. Wang, *Phys. Rev. B*, **33**, 8800 (1986).
20. J. P. Perdew, *Phys. Rev. B*, **33**, 8822 (1986).
21. G. I. Csonka and J. Réffy, *Chem. Phys. Lett.*, **229**, 191 (1994).
22. P. J. Stephens, F. J. Devlin, C. F. Chabalowski, and M. J. Frisch, *J. Phys. Chem.*, **98**, 11623 (1994).
23. G. I. Csonka and L. Sztraka, *Chem. Phys. Lett.*, **233**, 611 (1995).
24. (a) R. F. W. Bader, *Accts. Chem. Res.*, **9**, 18 (1985); (b) R. F. W. Bader, *Atoms in Molecules—A Quantum Theory*, Oxford University Press, Oxford, 1990.
25. U. Koch and P. L. A. Popelier, *J. Phys. Chem.*, **99**, 9747 (1995), and see references therein.
26. W. Koch, G. Frenking, J. Gauss, D. Cremer, and J. R. Collins, *J. Am. Chem. Soc.*, **109**, 5917 (1987).
27. R. F. W. Bader, T. S. Slee, D. Cremer, and E. Kraka, *J. Am. Chem. Soc.*, **105**, 5061 (1983).
28. C. Møller and M. S. Plesset, *Phys. Rev.*, **46**, 618 (1934).
29. A. D. Becke, *Phys. Rev. A*, **38**, 3098 (1988).
30. C. Lee, W. Yang, and R. G. Parr, *Phys. Rev. B*, **37**, 785 (1988).
31. A. D. Becke, *J. Chem. Phys.*, **98**, 5648 (1993).
32. M. J. Frisch, G. W. Trucks, M. Head-Gordon, P. M. W. Gill, M. W. Wong, J. B. Foresman, B. G. Johnson, H. B. Schlegel, M. A. Robb, E. S. Replogle, R. Gomperts, J. L. Andres, K. Raghavachari, J. S. Binkley, C. Gonzalez, R. L. Martin, D. J. Fox, D. J. DeFrees, J. Baker, J. J. P. Stewart, and J. A. Pople, Gaussian 92/DFT, Revision F, Gaussian, Inc., Pittsburgh, PA, 1993.
33. R. F. W. Bader's laboratory, AIMPAC, McMaster University, Hamilton, ON L8S 4M1, Canada.
34. G. Schultz, I. Hargittai, and R. Seip, *Z. Naturforsch.*, **36a**, 669 (1981).
35. M. Brewster, E. Pop, M.-J. Huang, and N. Bodor, *J. Mol. Struct. (Theochem)*, **303**, 25 (1994).
36. T. Clark, *A Handbook of Computational Chemistry*, Wiley, New York, 1985, p. 119.
37. D. J. DeFrees, B. A. Levi, S. K. Pollack, W. J. Hehre, J. S. Binkley, and J. A. Pople, *J. Am. Chem. Soc.*, **101**, 4085 (1979).
38. The *ZPVE* corrections are obtained from harmonic vibrational frequencies calculated at the HF/6-31G** level and are scaled by a factor of 0.89 in accord with known overestimates at this level (see ref. 60).
39. *ZPVE* corrections for saddle-points on the PES contain certain inaccuracy due to neglect of the contribution of the smallest (negative) vibrational frequency to the *ZPVE* by G92/DFT. For a 40 cm^{-1} vibration (the smallest frequency in **1d**) it takes 0.06 kcal/mol.
40. R. J. Gillespie and I. Hargittai, *The VSEPR Model of Molecular Geometry*, Allyn and Bacon, Boston, 1991.
41. W. J. Hehre, L. Radom, P. v. R. Schleyer, and J. A. Pople, *Ab Initio Molecular Orbital Theory*, Wiley, New York, 1986, p. 142.
42. After completion of these calculations we became aware of a recent theoretical work on the phenol-water system including some geometrical data for the phenol molecule, calculated at the MP2/6-31G** level (see ref. 61). The computed bond lengths in ref. 61 differ from ours in the third decimal only (up to two units).
43. A. Domenicano and I. Hargittai, Eds., *Accurate Molecular Structures*, Oxford University Press, Oxford, UK, 1992.
44. N. W. Larsen, *J. Mol. Struct.*, **51**, 175 (1979).
45. G. Portalone, G. Schultz, A. Domenicano, and I. Hargittai, *Chem. Phys. Lett.*, **197**, 482 (1992).
46. H. Konschin, *J. Mol. Struct. (Theochem)*, **92**, 173 (1983).
47. C. Puebla and T.-K. Ha, *J. Mol. Struct. (Theochem)*, **204**, 337 (1990).
48. C. W. Bock, M. Trachtman, and P. George, *J. Mol. Struct. (Theochem)*, **139**, 63 (1986).
49. C. W. Bock and I. Hargittai, *Struct. Chem.*, **5**, 307 (1994).
50. I. Hargittai, In *Stereochemical Applications of Gas-Phase Electron Diffraction, Part A*, I. Hargittai and M. Hargittai, Eds., VCH, New York, 1988, p. 1.
51. T. Schaefer and G. H. Penner, *J. Mol. Struct. (Theochem)*, **138**, 305 (1986).

52. A. Domenicano, In *Stereochemical Applications of Gas-Phase Electron Diffraction, Part B*, I. Hargittai and M. Hargittai, Eds., VCH, New York, 1988, Chapter 7.
53. (a) G. Gilli, F. Bellucci, V. Ferretti, and V. Bertolasi, *J. Am. Chem. Soc.*, **111**, 1023 (1989); (b) P. Gilli, V. Ferretti, V. Bertolasi, and G. Gilli, In *Advances of Molecular Structure Research*, M. Hargittai and I. Hargittai, Eds., JAI Press, Greenwich, CT, 1996, Vol. 2, pp. 67–102.
54. E. Vajda and I. Hargittai, *J. Phys. Chem.*, **96**, 5843 (1992).
55. G. Schultz and I. Hargittai, *J. Phys. Chem.*, **97**, 4996 (1993).
56. G. Schultz and I. Hargittai, *J. Phys. Chem.*, **99**, 11412 (1995).
57. K. B. Wiberg, In *Theoretical Models of Chemical Bonding, Part 1*, Z. B. Maksic, Ed., Springer-Verlag, Berlin, 1990, p. 255.
58. Our $\nabla^2\rho$ values for the *BCP* of the C—F bonds obtained at the HF/6-31G** level are in the range 0.20–0.28 a.u.
59. G. I. Csonka, N. Anh, J. Ángyán, and I. G. Csizmadia, *Chem. Phys. Lett.*, **245**, 129 (1995).
60. R. F. Hout, B. A. Levi, and W. J. Hehre, *J. Comput. Chem.*, **3**, 234 (1982).
61. D. Feller and M. Feyereisen, *J. Comput. Chem.*, **14**, 1027 (1993).